

Enhancement of ferroelectricity in Cr-doped $\text{Ho}_2\text{Ti}_2\text{O}_7$

X. W. Dong,¹ S. Dong,² K. F. Wang,¹ J. G. Wan,¹ and J.-M. Liu^{1,3,a)}

¹Laboratory of Solid State Microstructures, Nanjing University, Nanjing 210093, China

²Department of Physics, Southeast University, Nanjing 211189, China

³International Center for Materials Physics, Chinese Academy of Sciences, Shenyang 110016, China

(Received 20 March 2010; accepted 25 May 2010; published online 18 June 2010)

A series of polycrystalline pyrochlore rare-earth titanate $\text{Ho}_{2-x}\text{Cr}_x\text{Ti}_2\text{O}_7$ are synthesized in order to enhance the ferroelectricity of pyrochlore $\text{Ho}_2\text{Ti}_2\text{O}_7$. A giant enhancement of polarization P from $0.54 \mu\text{C}/\text{m}^2$ at $x=0$ up to $\sim 660 \mu\text{C}/\text{m}^2$ at $x=0.4$ is obtained, accompanied with an increment of ferroelectric transition point T_c from $T_c \sim 60$ K up to $T_c \sim 140$ K. A magnetic anomaly at $T_c \sim 140$ K together with the polarization response to magnetic field is identified, implying the multiferroic effect in $\text{Ho}_{2-x}\text{Cr}_x\text{Ti}_2\text{O}_7$. © 2010 American Institute of Physics.

[doi:10.1063/1.3455100]

Multiferroics, in which ferroelectric (FE) and spin orders coexist and couple with each other through magnetoelectric (ME) effect, have become a focus of many researches due to potential applications and challenges to fundamental physics.¹⁻³ Attentions have been paid to search for more multiferroics with high FE Curie point (T_c), large FE polarization (P), and intrinsic ME coupling.⁴⁻⁷ Recently, we reported the coexisting magnetic and FE behaviors in pyrochlore compound $\text{Ho}_2\text{Ti}_2\text{O}_7$ (HTO) below $T_c \sim 60$ K, although the measured P below temperature $T \sim 10$ K is very weak ($\sim 0.54 \mu\text{C}/\text{m}^2$).⁸

HTO is a member of materials with the general formula $\text{A}_2\text{B}_2\text{O}_7$, and crystallizes in pyrochlore structure (space group $Fd\bar{3}m$).⁹ The ideal pyrochlore structure can be considered as two independent frameworks ($\text{A}_2\text{O}'$ and B_2O_6), thus $\text{A}_2\text{B}_2\text{O}_7$ is often written as $\text{A}_2\text{B}_2\text{O}_6\text{O}'$ to distinguish the oxygen atoms of two different networks.¹⁰ As a spin-ice compound, $\text{Ho}_2\text{O}'$ sublattice [Fig. 1(a)] can be decomposed into two orthogonal sets of chains, which run along the orthogonal $[1\bar{1}0]$ and $[110]$ directions, respectively. At low- T , Ho^{3+} cations occupy the corner sites of tetrahedra, whose easy spin axes point to the centers of tetrahedra (the local $\langle 111 \rangle$ directions), as shown in Fig. 1(b).

A well-confirmed fact is that the A cation must be appreciably larger than the B cation in this structure.^{10,11} A distortion of the $[\text{BO}_6]$ octahedral will be induced if the radius of A cation is small. Such lattice distortion is very impacting on the FE behaviors of multiferroics. Therefore, one can dope small cation at the A site to modulate (enhance) the lattice distortion, then to enhance the ferroelectricity. As for HTO, the radius of Ho^{3+} ($r=0.901 \text{ \AA}$) is extremely large (noting $r=0.605 \text{ \AA}$ for Ti^{4+}), thus allowing an opportunity to modify HTO in terms of the ferroelectricity improvement. In order to induce a large lattice distortion, we choose small magnetic ions Cr^{3+} ($r=0.615 \text{ \AA}$) to substitute Ho^{3+} in HTO, while earlier works only dealt with the different rare-earth ions substitution at A sites.^{12,13}

Moreover, the magnetic ion Ho^{3+} in HTO carries a large magnetic moment ($\sim 10 \mu_B$), such that the long-range magnetic dipolar interaction is as significant as the nearest-

neighbor exchange.¹⁴ While the spin moment of Cr^{3+} ($\sim 3 \mu_B$) is much smaller than Ho^{3+} , such a substitution would weaken the long-range magnetic dipolar interactions, and may allow the nearest-neighbor exchange to be dominant, thus offering a different magnetic behavior in Cr-doped HTO. This is another focus of our work. We will investigate the FE and magnetic properties of $\text{Ho}_{2-x}\text{Cr}_x\text{Ti}_2\text{O}_7$ (HCTO).

Polycrystalline HCTO samples were synthesized by solid state reaction. The phase purity was checked by x-ray diffraction (XRD) using $\text{Cu K}\alpha$ radiation and transmission electron microscopy (TEM). The T - and magnetic field (H) dependences of magnetization (M) were measured using the superconducting quantum interference device magnetometer (Quantum Design, Inc.). For measuring P , we detected the

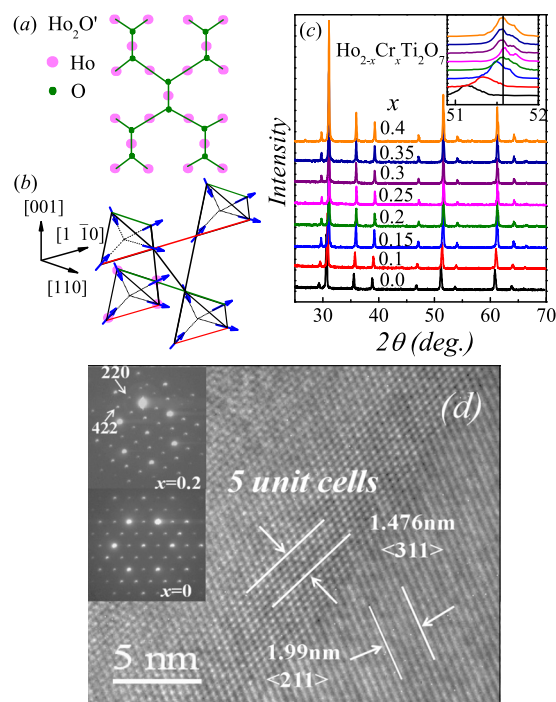


FIG. 1. (Color online) (a) Planar view of $\text{Ho}_2\text{O}'$ sublattice along the $[110]$ and (b) spin structure of HTO. (c) XRD patterns of HCTO at $x < 0.5$. (d) TEM image ($x=0.2$), with the incident beam parallel to $[111]$ and the insets are the selected area electron-diffraction patterns ($x=0$ and 0.2) with the incident beams parallel to $[111]$.

^{a)} Author to whom all correspondences should be addressed. Electronic mail: liujm@nju.edu.cn.

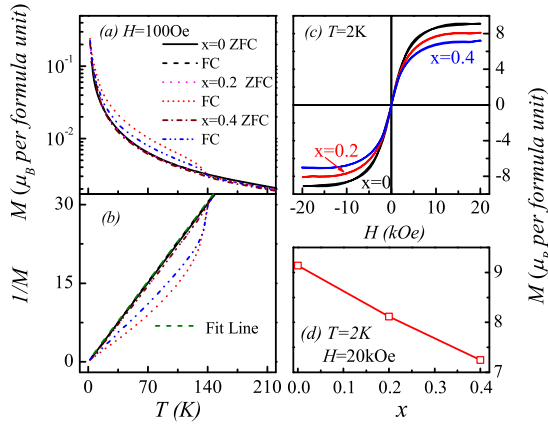


FIG. 2. (Color online) (a) Measured $M(T)$ and (b) $1/M(T)$ dependences under the ZFC and FC sequences for $x=0, 0.2$, and 0.4 . (c) Measured M - H hysteresis for $x=0, 0.2$, and 0.4 at $T=2$ K. (d) Saturated M as a function of x .

pyroelectric current (I) using an electrometer (Keithley 6514) associated with the physical property measurement system. The poling electric field is $E=5$ kV/cm. The FE hysteresis was also evaluated by a systematic measurement of the pyroelectric current and polar-switching current upon reversal of electric field.

First, the XRD θ - 2θ spectra data for eight HCTO samples at different x are presented in Fig. 1(c). It indicates that the samples all have the single-phase pyrochlore structure and no impurity peak is identified. The reflection peaks shift toward the high θ side with increasing x and the structure becomes stable after a continuous lattice contraction until $x=0.2$, as shown in the inset of Fig. 1(c). This is reasonable, noting that Cr ion is smaller than Ho ion. In addition, the Cr-doping seems to induce a weak shoulder appearing at the immediate right-side of the main peak between $2\theta=51^\circ$ and 52° , indicating the continuously enhanced lattice distortion with increasing x , while details of the lattice symmetry breaking if any remain unclear so far.

We also show the TEM observation to support the XRD results, and one example for $x=0.2$ is shown in Fig. 1(d). The TEM selected area electrodiffraction patterns with the incident beam parallel to the $[111]$ orientation are presented in the inset of Fig. 1(d). By a careful examination, halos in the pattern of HCTO $x=0.2$ are observable with respect to that of HTO, which means that the crystal structure is distorted by Cr-doping. In addition, the evaluated interplane separation d of $\langle 220 \rangle$, $\langle 422 \rangle$, $\langle 311 \rangle$, and $\langle 211 \rangle$ are, respectively, 3.48 Å, 2.04 Å, 2.952 Å, and 3.98 Å, which are smaller than that of pure HTO ($d=3.57, 2.06, 3.05$, and 4.12 Å for $\langle 220 \rangle$, $\langle 422 \rangle$, $\langle 311 \rangle$, and $\langle 211 \rangle$ of HTO).

Subsequently, we characterize the magnetic and FE behaviors. We look at the magnetism of several samples, noting that HTO is a spin ice.¹⁵ Figure 2(a) shows the M - T curves measured under $H=0.01$ T for both zero-field cooled (ZFC) and field-cooling (FC) conditions. For HTO, no significant difference between the ZFC and FC curves is observed, indicating that the spin-ice configuration is quite robust. However, for $x=0.2$ and 0.4 , the ZFC and FC curves show a clear separation at $T \sim 140$ K upon decreasing T , which is a surprising anomaly, to be addressed below. If using the Curie-Weiss law to fit the data, one observes a roughly good paramagnetic behavior for HTO even down to $T \sim 2$ K,

indicating the typical spin-ice behavior, as shown by the dashed line in Fig. 2(b). For $x=0.2$ till $x=0.4$, observation reveals not only the aforesaid anomaly, but also a departure of the ZFC curve from the fitting line, initiating at $T \sim 140$ K. This departure indicates that the spin-ice configuration of HCTO is not as robust as that of HTO in response to H .

To understand this anomaly, we consult to the spin structure. For HTO, the Ho spins are characterized by the effective classical Ising spins constrained to the local $\langle 111 \rangle$ directions below $T \sim 200$ K.¹⁵ As a gradual sequence, the Ho spins will be ordering into the “two-in–two-out” alignment at low- T . For HCTO, Cr^{3+} ions replace partial Ho^{3+} ions, resulting in the weakening of the local trigonal crystal field and the long-range magnetic dipolar interactions responsible for the spin ice behavior. This may lead to the appearance of the “three-in–one-out” state, or the local “two-in–two-out” state can be easily changed into the “three-in–one-out” state, driven by, e.g., magnetic field.^{16–18} Noting that the “three-in–one-out” state has larger magnetization than the “two-in–two-out” state along the $[111]$ direction, one then understands that for HCTO the slight deviation of the M - T curves from the Curie-Weiss law at $T < 140$ K is due to partial activation of the “three-in–one-out” state by the measuring H . This explains why the spin ice configuration of HCTO is less stable than that of HTO. Furthermore, the slight decrease in M with increasing x at low- T [Fig. 2(d)] is due to the smaller moment of Cr^{3+} than Ho^{3+} , although the “three-in–one-out” state may have slightly larger M than the “two-in–two-out” state. The measured M - H loops at $T \sim 2$ K for $x=0, 0.2$, and 0.4 , are shown in Fig. 2(c). It is noted that M becomes almost saturated at $H > 1.0$ T and the coercive field is very small, a typical feature for spin ice system too.

Finally, we look at the ferroelectricity. The data reliability is evidenced by the $I(T)$ curves under different warming ramp rates and one example for HCTO $x=0.2$ at the rate of 2 and 4 K/min is given in Fig. 3(a), excluding the possible contribution from any trapped charges. Figure 3(b) shows the T -dependence of P for various HCTO samples, with $E=5$ kV/cm. For HTO, one can see that the FE transition appears at $T \sim 60$ K. The maximum P is only $\sim 0.54 \pi\text{C}/\text{m}^2$, quite small with respect to other multiferroics. However, for HCTO at $x > 0.1$, the P is remarkably enhanced, as also seen in the inset of Fig. 3(b) which shows the x -dependence of P at $T \sim 10$ K. Here, it is noted that P at $x=0.1$ is enhanced up to $\sim 1.9 \mu\text{C}/\text{m}^2\text{c}$. Above $x > 0.1$, P increases rapidly and reaches a value as high as $660 \mu\text{C}/\text{m}^2$ at $x=0.4$, which is almost 1200 times as that of HTO. The measured T_c for HCTO $x=0.4$ is ~ 140 K. The inset of Fig. 3(b) shows that T_c increases with x below $x < 0.2$ and tends to be less sensitive to x at $x > 0.2$.

Moreover, it is noted that the ferroelectricity generation is roughly coincident with the anomaly of the M - T curves, implying the ME effect. This can be further confirmed by the T -dependence of $\Delta P = P(H) - P(H=0)$ for $x=0.4$, and the data under $H=1.0, 3.0$, and 9.0 T are shown in Fig. 3(c). ΔP increases with increasing H , demonstrating the significant response of P against H , i.e., the multiferroicity. However, the measured ΔP becomes less sensitive to H as $H > 3.0$ T. The inset of Fig. 3(c) shows the measured P - E hysteresis for HCTO $x=0.4$ at $T \sim 10$ K, where electric field E is ramping between ± 10 kV/cm.

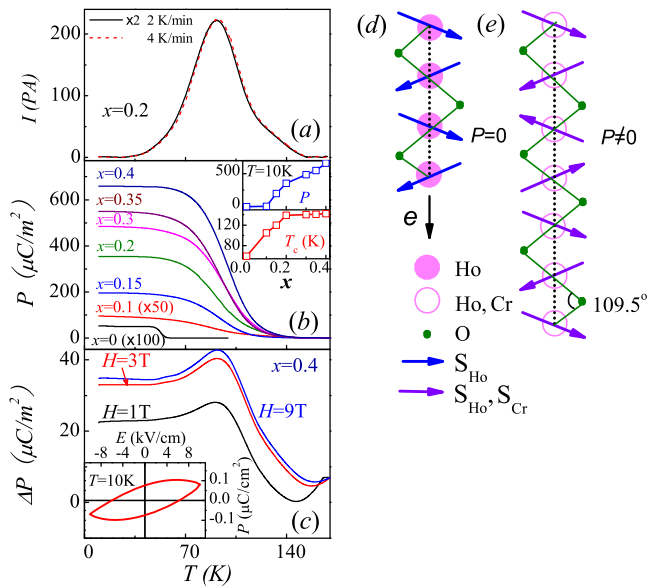


FIG. 3. (Color online) (a) Measured $I(T)$ at two warming ramp rates (2 and 4 K/min) for $x=0.2$. (b) Measured $P(T)$ for several samples and the insets are $P(x)$ at $T \sim 10$ K and $T_c(x)$. (c) $\Delta P = P(H) - P(H=0)$ as a function of T for $x=0.4$ under $H=1.0$ T, 3.0 T, and 9.0 T, respectively, and the inset shows the P - E loop at $T \sim 10$ K. (d) A sketch of one $\text{Ho}_2\text{O}'$ chain with the Ho-O-Ho bond angle of 109.5° . (e) A sketch of one possible $\text{Ho}(\text{Cr})\text{-O-Ho}(\text{Cr})$ chain generating nonzero P .

Based on the above results, we are allowed to clarify the origin of P for HCTO. It seems that both the TiO_6 octahedra due to the lattice distortion and the Ho spin chains can contribute to the ferroelectricity, which allows us to propose the two possible mechanisms. First, the Cr-doping results in lattice shrinking and distortion of the $[\text{TiO}_6]$ octahedral and thus the relative shift of Ti^{4+} ions from surrounding oxygen ions. This effect contributes to ferroelectricity generation, via the classical soft-mode mechanism. The TO_4 mode excitation if any may evidence this picture.^{19,20}

Second, the contribution of inverse Dzyaloshinskii-Moriya interaction (DMI) to the ferroelectricity should also be taken into account (DMI mechanism).²¹ We show the Ho-O-Ho chain of HTO with the Ho spins in Fig. 3(d) where the oxygen shift from the Ho chain axis is exaggerated for clarification consideration. It is seen that the local DMI may also contribute to a local electric polar moment. However, the overall polar moment is zero due to the interpole cancel along the Ho-O-Ho chain.²² For HCTO, the continuous Ho-O-Ho chain is broken due to the Cr-doping and the “three-in-one-out” alignment can be induced, generating a spin configuration different from that shown in Fig. 3(d). One possible configuration is given in Fig. 3(e) where the overall inter-pole cancel becomes unsatisfied, generating the net nonzero polarization.

A combination of the two mechanisms can explain qualitatively the observed results, although this combined model is over-simplified without including the correlation between them. First, the two mechanisms both contribute to the enhanced FE T_c with x until $x \sim 0.2$ at which $T_c \sim 140$ K. The less sensitivity of T_c to x as $x > 0.2$ can be partially explained by the fact that the lattice shrinking and distortion become less sensitive to x as $x \sim 0.2$. In addition, the observed mag-

netic anomaly associated with the “three-in-one-out” spin state in coexistence with the “two-in-two-out” spin state occurs at $T \sim 140$ K, implying that the DMI mechanism for polarization is active at $T < 140$ K. Both the effects lead to the observed $T_c(x)$ shown in the inset of Fig. 3(b). Second, for $x > 0.2$, the DMI mechanism is mainly responsible for the continuous enhancement of P with x , noting that additional lattice shrinking and distortion are less pronounced.

The response of P to H should be solely attributed to the DMI mechanism. If $M(H)$ becomes saturated above certain H value, one may expect no more further response of P to H . Thus, it is understandable to observe no much difference in P measured at $H=3$ and 9 T in the low- T range. However, the measured M decreases slowly with increasing T , and the critical H required for a “saturated” M is also larger for a higher T (e.g., $H > 4.0$ T at $T=60$ K). At $T > 80$ K, no saturated M can be observed due to the gradually enhanced paramagnetic signals at high T . This requires more investigation on the mechanism for $P(H)$ behavior in the high- T range.

This work was supported by the National Natural Science Foundation of China (Grant Nos. 50832002 and 10874075), the National Key Projects for Basic Researches of China (Grant Nos. 2009CB623303 and 2006CB921802), and the Natural Science Foundation of China in Jiangsu (Grant No. BK2008024).

¹M. Fiebig, *J. Phys. D: Appl. Phys.* **38**, R123 (2005).

²K. F. Wang, J.-M. Liu, and Z. F. Ren, *Adv. Phys.* **58**, 321 (2009).

³S.-W. Cheong and M. Mostovoy, *Nature Mater.* **6**, 13 (2007).

⁴J. Y. Park, J. H. Park, Y. K. Jeong, and H. M. Jang, *Appl. Phys. Lett.* **91**, 152903 (2007).

⁵D. Meier, M. Maringer, T. Lottermoser, P. Becker, L. Bohaty, and M. Fiebig, *Phys. Rev. Lett.* **102**, 107202 (2009).

⁶J. S. Lee, N. Kida, S. Miyahara, Y. Takahashi, Y. Yamasaki, R. Shimano, N. Furukawa, and Y. Tokura, *Phys. Rev. B* **79**, 180403(R) (2009).

⁷S. J. Luo, K. F. Wang, S. Z. Li, X. W. Dong, Z. B. Yan, H. L. Cai, and J.-M. Liu, *Appl. Phys. Lett.* **94**, 172504 (2009).

⁸X. W. Dong, K. F. Wang, S. J. Luo, J. G. Wan, and J.-M. Liu, *J. Appl. Phys.* **106**, 104101 (2009).

⁹J. P. Clancy, J. P. C. Ruff, S. R. Dunsiger, Y. Zhao, H. A. Dabkowska, J. S. Gardner, Y. Qiu, J. R. D. Copley, T. Jenkins, and B. D. Gaulin, *Phys. Rev. B* **79**, 014408 (2009).

¹⁰T. A. Vanderah, I. Levin, and M. W. Lufaso, *Eur. J. Inorg. Chem.* **2005**, 2895 (2005).

¹¹L. Minervini and R. W. Grimes, *J. Am. Ceram. Soc.* **83**, 1873 (2000).

¹²X. Ke, D. V. West, R. J. Cava, and P. Schiffer, *Phys. Rev. B* **80**, 144426 (2009).

¹³H. Xing, M. He, C. M. Feng, H. J. Guo, H. Zeng, and Z.-A. Xu, *Phys. Rev. B* **81**, 134426 (2010).

¹⁴R. Siddharthan, B. S. Shastry, A. P. Ramirez, A. Hayashi, R. J. Cava, and S. Rosenkranz, *Phys. Rev. Lett.* **83**, 1854 (1999).

¹⁵S. T. Bramwell and M. J. P. Gingras, *Science* **294**, 1495 (2001).

¹⁶M. J. Harris, S. T. Bramwell, P. C. W. Holdsworth, and J. D. M. Champion, *Phys. Rev. Lett.* **81**, 4496 (1998).

¹⁷H. Fukazawa, R. G. Melko, R. Higashinaka, Y. Maeno, and M. J. P. Gingras, *Phys. Rev. B* **65**, 054410 (2002).

¹⁸T. Katsufuji and H. Takagi, *Phys. Rev. B* **69**, 064422 (2004).

¹⁹A. Durán, E. Martínez, J. A. Díaz, and J. M. Siqueiros, *J. Appl. Phys.* **97**, 104109 (2005).

²⁰R. Garg, A. Senyshyn, H. Boysen, and R. Ranjan, *Phys. Rev. B* **79**, 144122 (2009).

²¹I. A. Sergienko and E. Dagotto, *Phys. Rev. B* **73**, 094434 (2006).

²²H. Katsura, N. Nagaosa, and A. V. Balatsky, *Phys. Rev. Lett.* **95**, 057205 (2005).